Earth and Planetary Science Letters 365 (2013) 209–220

Contents lists available at SciVerse ScienceDirect

Earth and Planetary Science Letters

journal homepage: www.elsevier.com/locate/epsl

Constraints on melting processes and plume-ridge interaction from comprehensive study of the FAMOUS and North Famous segments, Mid-Atlantic Ridge

Allison Gale*, Muriel Laubier, Stéphane Escrig, Charles H. Langmuir

Department of Earth and Planetary Sciences, Harvard University, 20 Oxford Street, Cambridge, MA 02138, USA

ARTICLE INFO

Article history:
Received 15 December 2011
Received in revised form
15 January 2013
Accepted 19 January 2013
Editor: T. Elliott
Available online 28 February 2013

Keywords:
FAMOUS
mid-ocean ridge basalt
trace element geochemistry
plume–ridge interaction

ABSTRACT

Detailed major element, trace element and isotopic study of the FAMOUS and North Famous segments within the geochemical gradient south of the Azores platform provides new constraints on controls on chemical variations at the segment scale and the origin of plume geochemical gradients. A comprehensive investigation of 110 samples along the entire length of the FAMOUS segment, coupled with a recent extensive melt inclusion study by Laubier et al. (2012), shows large trace element diversity within a single segment and substantial isotopic variability that largely correlates with trace element variations. Substantial variations are also present along the short (18 km) North Famous segment despite the presence of an axial volcanic ridge. These results confirm multiple supply of magmas along the length of these segments, the lack of a centrally supplied magma chamber, and the ability of melting processes to deliver highly diverse melts over short distances and times. With the exception of one group of high Al_2O_3, low SiO_2 magmas (HiAl–LoSi) largely recovered in the original small FAMOUS area, the data can be simply explained by a two-component mixing model coupled with melting variations. The HiAl–LoSi magmas reflect assimilation and mixing in the crust, an interpretation supported by the diverse melt inclusions in these lavas.

Since the mantle heterogeneity reflects two-component mixing, the end members can be constrained. Surprisingly, source mixing between the Azores plume and depleted mantle cannot produce the observations. This is evident regionally from the fact that nearly all basalts have highly incompatible trace element ratios (e.g., Th/La, Nb/La) as high or higher than the most plume-influenced MORB near the Azores hotspot, despite being over 300 km farther south and much less enriched isotopically. To account for the elevated highly incompatible trace element ratios, a metasomatic component formed by adding deep, low-degree melts of Azores plume material to a depleted mantle is required. The regional gradient south of the Azores then requires different processes along its length. Close to the Azores, plume material mixes with depleted mantle. The pure plume influence is spatially restricted, and enrichment farther to the south is caused by shallow mantle metasomatized by low-degree melts from deep plume flow. North Famous lavas are spatially closer to the Azores and yet are more depleted in trace elements and isotopes than FAMOUS lavas, suggesting delivery of the enriched component to individual segments is influenced by additional factors such as segment size and offset. The extent to which these processes operate in other regions of plume–ridge interaction remains to be investigated.

1. Introduction

Detailed, segment-scale studies of ocean ridges provide opportunities to address major questions of ocean ridge petrogenesis that cannot be investigated using only regional - scale sampling. Such opportunities are enhanced for segments within a regional gradient in composition. For example, gradients in ridge geochemistry and bathymetry near mantle plumes have long been suggested to result from mixing between enriched and depleted mantle sources in the solid state (e.g., Schilling, 1975, 1983; Dosso et al., 1999), or more recently, from preferential melting of enriched veins from a homogeneous source during active upwelling (Ito and Mahoney, 2005a, 2005b). Most of the data for these arguments has been based on regional sampling (a few samples per segment). Highly detailed sampling within individual segments provides an important additional perspective, by showing the mixing end members and melting processes that vary on a small temporal and spatial scale.

The FAMOUS ("French American Mid-Ocean Undersea Study") segment of the Mid-Atlantic Ridge (MAR) provides an ideal study

* Corresponding author. Tel.: +1 617 496 8418; fax: +1 617 496 6958.
E-mail address: agale@fas.harvard.edu (A. Gale).

0012-821X/$ - see front matter © 2013 Elsevier B.V. All rights reserved.
http://dx.doi.org/10.1016/j.epsl.2013.01.022

location because of its exceptionally high sampling density. Initial sampling focused on the 'FAMOUS area', an area a few km^2 just north of the segment center, and then another small region at the segment center, called 'Narrowgate' because of the narrow rift valley that occurs there. Over the years a substantial number of dredges and rock cores have provided additional coverage along the entire length of the segment. As a result of such sampling, many studies have discussed the petrogenesis of these lavas (e.g., Bougault and Hékinian, 1974; Bougault et al., 1984; Bryan, 1979; Bryan and Moore, 1977; Frey et al., 1993; Kamenetsky, 1996; Langmuir et al., 1977; Laubier et al., 2007, 2012; le Roex et al., 1981, 1996; Shimizu, 1998; Stakes et al., 1984; White and Bryan, 1977). Bryan and Moore (1977), using major element chemistry, suggested that FAMOUS area basalts were derived from a single magma chamber. Langmuir et al. (1977) showed that trace element variations were too large to be explained by magma chamber processes, and argued that dynamic melting of a homogeneous source region better accounted for the data, and that large magma chambers did not exist. Stakes et al. (1984) used petrographic observations and major element compositions of Narrowgate lavas farther south to again suggest that shallow magma chamber processes could account for their compositional diversity. Frey et al. (1993) later demonstrated that crustal processes could not account for the trace element chemistry (e.g., highly variable La/Yb ratios) of the Narrowgate lavas, and instead proposed more complex partial melting processes to explain the data.

These early studies assumed a homogeneous mantle source based on isotopic data that showed little resolvable variation (e.g., Frey et al., 1993; White and Bryan, 1977). Three isotopic measurements of Narrowgate samples by le Roex et al. (1996) showed isotopic differences that they interpreted to reflect a temporal change in the composition of mantle beneath the segment. Within each temporal group, however, they argued for dynamic melting processes to account for the data.

None of these studies made use of the entire available set of samples from the French and American collections, were able to consider variations on a segment scale, or interpreted the data in the context of the regional gradient south of the Azores (Schilling, 1975). Nearly all of them also took place prior to the advent of modern ICP-MS techniques for collecting trace element data. The present study offers a more comprehensive view by including samples from over 110 unique locations from the French and American collections, and by reporting new major element, ICP-MS trace element and Sr–Nd–Pb isotopic analyses on basaltic glasses. A parallel major and trace element study of over 300 olivine-hosted melt inclusions from multiple samples from the FAMOUS segment (Laubier et al., 2012) provides additional insights into mantle melting and crustal processes occurring along the segment. The sheer number of samples analyzed with consistent laboratory techniques, and the ability to compare results with such a comprehensive melt inclusion study, make this the single most extensive study of its kind of a MAR segment.

A dataset of this magnitude permits exploration of questions such as the extent of chemical variation along a single segment, and the relative roles of mantle heterogeneity, partial melting and crustal processing in determining lava compositions. Another interesting aspect stems from the location of the FAMOUS segment within the geochemical gradient south of the Azores (Dosso et al., 1999; Schilling, 1975; White and Schilling, 1978). Basalts from ridge segments near the Azores are enriched in isotopes and highly incompatible elements, and this enrichment lessens southward. Our new data on the FAMOUS and North Famous (N. Famous) segments, coupled with recent data published by Gale et al. (2011) on the next two segments north (Lucky Strike "LS" and Menez Gwen "MG"; Fig. 1), constrain the origin of the

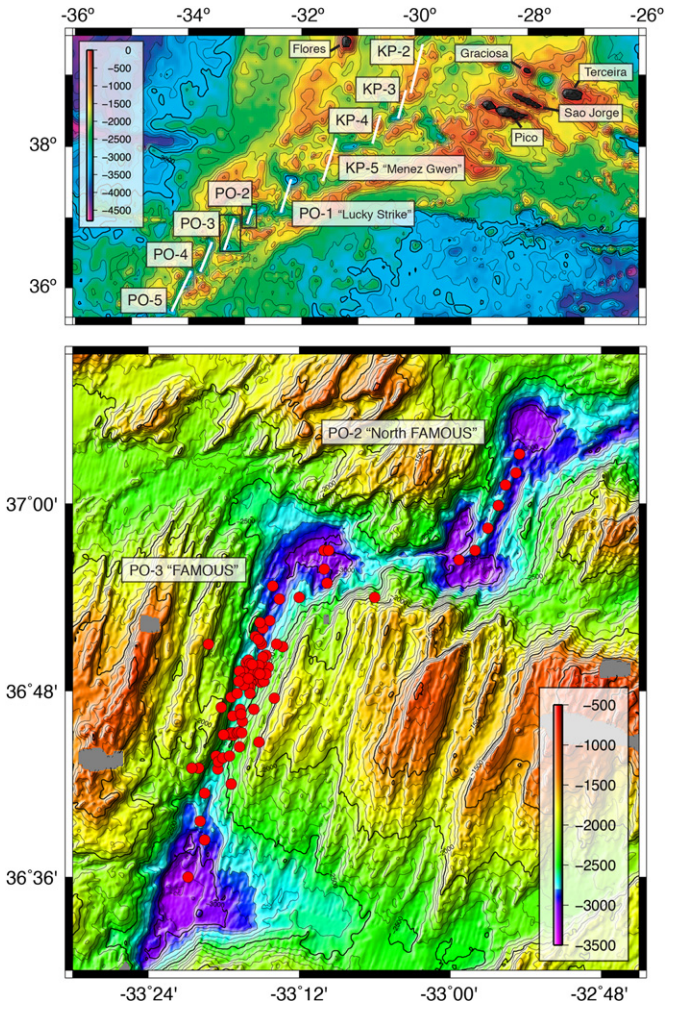

Fig. 1. Bathymetric map of the northern Mid-Atlantic Ridge, with detailed maps of the FAMOUS (PO-3) and North Famous (PO-2) segments showing the location of samples in this study. Labeled segments (indicated by white lines in regional map) follow the nomenclature of Detrick et al. (1995). Note the extensive sampling of the FAMOUS segment. A multibeam bathymetry grid (300 m spacing; Cannat et al., 1999; Escartin et al., 2001) was used for the detailed maps. Global multi-resolution bathymetry as compiled by Ryan et al. (2009) was used for the regional map (bathymetry in meters).

'regional gradient' associated with plume–ridge interaction. Gale et al. (2011) suggested that the geochemical gradient south of the Azores to LS is not caused by simple mixing between 'plume' mantle and 'depleted' mantle. Data from the segments farther south test this suggestion and provide additional constraints on how mantle plumes interact with the upper mantle to create geochemical gradients around hot spots.

2. Regional setting

Ridge segments south of the Azores were defined by Detrick et al. (1995) (Fig. 1). There is a marked bathymetric gradient southwards. The shallowest segments (KP-2 and KP-3) near 39°N have the most plume-like isotopic signature (Dosso et al., 1999). Just to the south are the MG (KP-5) and LS (PO-1) segments with robust axial volcanoes (Langmuir et al., 1997; Ondreas et al., 1997) recently studied by Gale et al. (2011). The N. Famous (PO-2) and FAMOUS (PO-3) segments are directly south of the LS segment (Fig. 1), and are the primary focus of the present study.

The FAMOUS segment (containing the small FAMOUS area) is 45 km long, bounded by 25 km offsets from the adjacent AMAR and N. Famous segments to south and north. Based on its mantle Bouguer anomaly, Detrick et al. (1995) suggest 3 km thicker crust at the segment center than segment ends. The segment varies from 2500 m depth at its shallowest point to >3000 m at the segment ends. The rift valley is marked by individual, small volcanic centers on the rift valley floor, and no clearly defined axial volcanic ridge (Ballard et al., 1975). The individual cones are separate volcanic edifices with distinct chemical compositions (Langmuir et al., 1977).

The N. Famous segment (Fig. 1) is the shortest (<18 km) segment from this portion of the MAR, with a depth gradient from 2700 m at segment center to 3100 m at segment ends, and 3 km crustal thickness variations estimated from gravity (Detrick et al., 1995). The mean depth of N. Famous (2880 m) is greater than FAMOUS (2670 m), breaking the trend of shallowing segments as the Azores platform is approached. In contrast to the isolated cones that mark the center of the FAMOUS segment, N. Famous has a well-developed axial volcanic ridge extending three quarters of its length.

3. Results

We report 105 new major element analyses, 145 new trace element analyses and 43 new isotope analyses from the FAMOUS and N. Famous segments (all analyses reported in Tables S1, S2 and S3). Full analytical details can be found in the Supplementary material. "New" analyses are either on new samples or are reanalyses of previously measured samples. For this study, we carried out a systematic determination of interlaboratory bias factors so the abundant major element data from the Smithsonian (Melson et al., 2002) could be readily included (see Supplementary material for details). In order to obtain trace elements on the Smithsonian microprobe mounts, some laser ablation ICP-MS data were collected along with solution ICP-MS analyses.

In the discussion below we use the terminology defined by Gale et al. (2013). Enriched MORB (E-MORB) are samples with $La/Sm_N > 1.5$. In contrast, depleted MORB (D-MORB) are characterized by more depleted compositions (e.g., $La/Sm_N < 0.8$). Transitional MORB (T-MORB) are intermediate in composition.

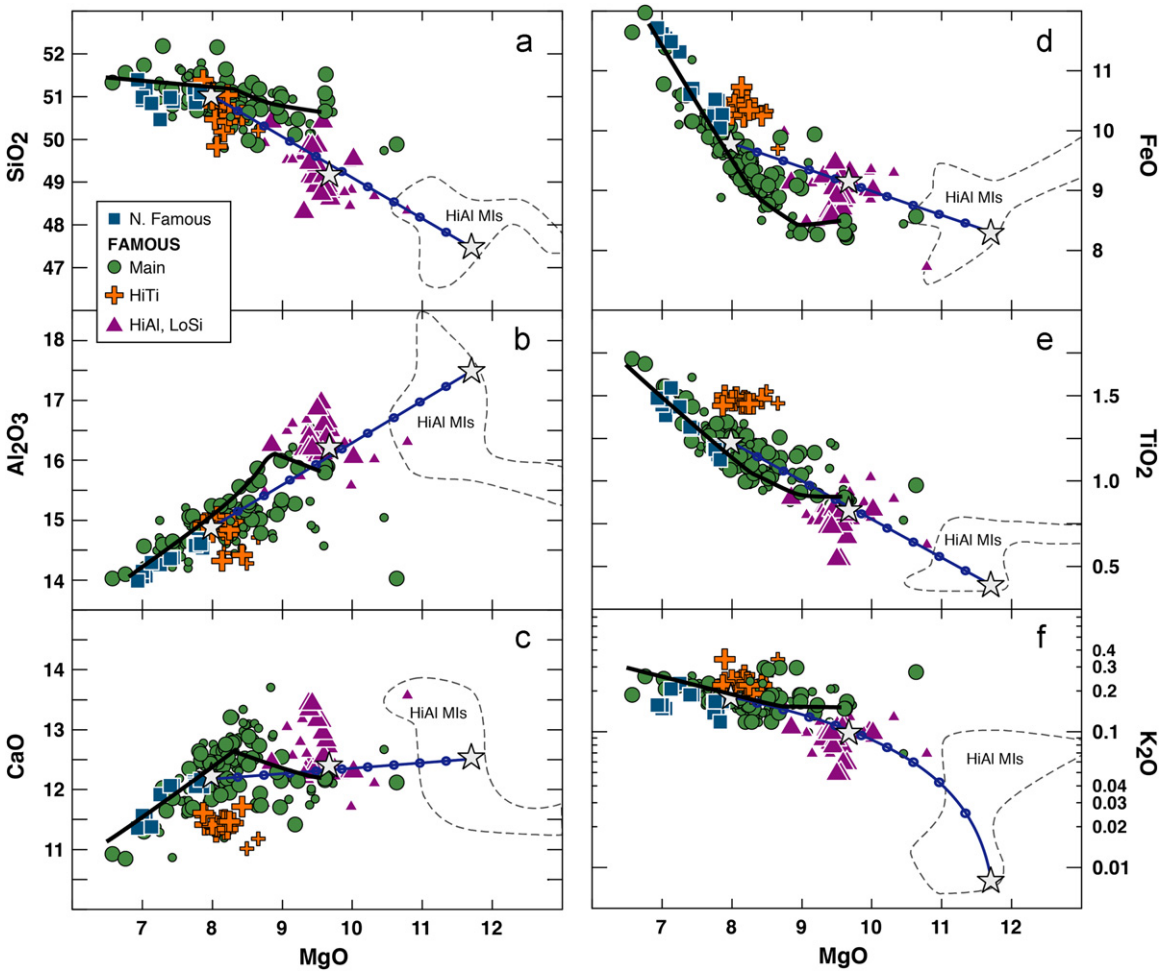

Fig. 2. (a–f) SiO_2, Al_2O_3, CaO, FeO, TiO_2 and K_2O vs. MgO. Smaller symbols indicate data already published (Bryan, 1979; Bryan and Moore, 1977; Kamenetsky, 1996; Melson et al., 2002; Sigurdsson, 1981; Stakes et al., 1984). N. Famous has one major element group, and its basalts are noticeably more fractionated than those from FAMOUS. In the FAMOUS segment there are three major element groups: Main, HiAl–LoSi and HiTi. There is a remarkable diversity of major element compositions seen in basalts from the FAMOUS segment. Of particular note is the preponderance of primitive (>9 wt% MgO) samples. More than one parental magma is required to explain the chemical variation seen at a given MgO content, but crystal fractionation has also been important in diversifying the compositions (see black line indicating a representative liquid line of descent from Bézos et al., in preparation). Also shown are fields for HiAl melt inclusions from the FAMOUS segment (Laubier et al., 2012). Mixing a representative HiAl melt inclusion and the average Main lava in 50:50 proportions accounts well for the major (and trace) element characteristics of the average HiAl–LoSi basalt (see dark blue curve with dots indicating 10% mixing increments; gray stars indicate the composition of the representative HiAl melt inclusion, the average HiAl–LoSi basalt and the average Main lava). (For interpretation of the references to color in this figure legend, the reader is referred to the web version of this article.)

3.1. Major elements

The major element data from the FAMOUS segment cover a wide range of compositions from <7 to >10 wt% MgO, coupled with factor of three variations in TiO_2 and factor of six variations in K_2O (Fig. 2). Three major element groups are noteworthy.

(1) The "high-Al_2O_3, low SiO_2 group" (HiAl–LoSi) has unusually high Al_2O_3 (15.75–17 wt%) and MgO (9–11 wt%), low SiO_2 (48–50 wt%) and low K_2O (<0.11 wt%). These basalts have characteristics similar to the high-Al_2O_3 basalts found along the Galapagos spreading center (Eason and Sinton, 2006). K_2O and TiO_2 contents vary by a factor of two.
(2) The dominant group of the FAMOUS segment (hereafter referred to as "Main") has MgO largely between 7 and 9 wt%, TiO_2 between 0.9 and 1.6 wt%, Al_2O_3 from 14 to 16 wt% and SiO_2 from 50 to 52 wt%. This group has characteristics similar to the T-MORB from the nearby LS segment (Gale et al., 2011).
(3) The "high TiO_2" group (HiTi), has a narrow MgO range (7.8–8.8 wt%) with higher TiO_2 (1.42–1.52 wt%) than the Main group. HiTi basalts are also noticeably higher in FeO (10.2–10.8 wt%) and K_2O and lower in CaO relative to the Main lavas.

The N. Famous segment has only one major element group and is generally more fractionated, with no lava having more than 7.9 wt% MgO. This contrasts with the FAMOUS segment, where there is a large population of primitive MORB.

Variation within the groups is also important. Crystal fractionation has played a role in diversifying the lava compositions, as evident from the calculated liquid lines of descent shown in Fig. 2 (liquid lines of descent from hBasalt; Bézos et al., in preparation). There are also differences within the groups that cannot be attributed to crystal fractionation. For example, K_{90}, the concentration of K_2O corrected for fractionation to be in equilibrium with Fo_{90} olivine, hereafter referred to as a "90-value" (details of fractionation correction in Supplementary material), varies from 0.1 to 0.25 in the Main group at FAMOUS.

3.2. Trace elements

Trace element variations are large in the FAMOUS area (Fig. 3), as known previously. The large variations result from the coexistence of E-MORB and the HiAl–LoSi lavas with low trace element concentrations (e.g., Nb_{90}, Ti_{90}) and moderate depletion in some trace element ratios (e.g., La/Sm). Despite the large variations in abundances (e.g., Ba_{90} abundances change by a factor of 6), there is a relative homogeneity of the ratios of the most highly incompatible elements. For example, most HiAl–LoSi samples and Main samples have Th/La between 0.095 and 0.11 as La/Sm varies by a factor of two. This observation is apparent from the similar shapes of the spidergrams in Fig. 3 for all elements more incompatible than Ce.

A notable contrast among the different sample groups, however, is in the slope of their HREE patterns. This can be observed in Fig. 3 from the upward sloping patterns of the HiAl–LoSi lavas from Sm to Yb, and the downward sloping patterns for the other sample groups. A convenient ratio illustrating this contrast is the Dy/Yb ratio. The HiAl–LoSi samples have similar Th/La ratios to the Main lavas, but are distinguished by subchondritic Dy/Yb ratios (<1.5; see Fig. S3 in supplementary material). Even lower Dy/Yb ratios are seen in HiAl olivine-hosted melt inclusions from FAMOUS (Laubier et al., 2012). This middle to heavy REE depletion coupled with enriched ratios of the most incompatible elements is fundamental to these lavas. A few of the most depleted HiAl–LoSi basalts from near the northern fracture zone boundary are also marked by positive Sr anomalies and slight positive Eu anomalies. This feature is shared by some of the melt inclusions reported in Laubier et al. (2012).

The Main lavas are all either flat or sloping downwards from Sm to Yb, in some cases crossing over the patterns of the HiAl–LoSi samples (Fig. 3). They exhibit a similar pattern to the HiAl–LoSi samples in the elements Ba through Sm, but offset to higher absolute concentrations. The most enriched samples in the FAMOUS segment, including E-MORB, are in the Main group.

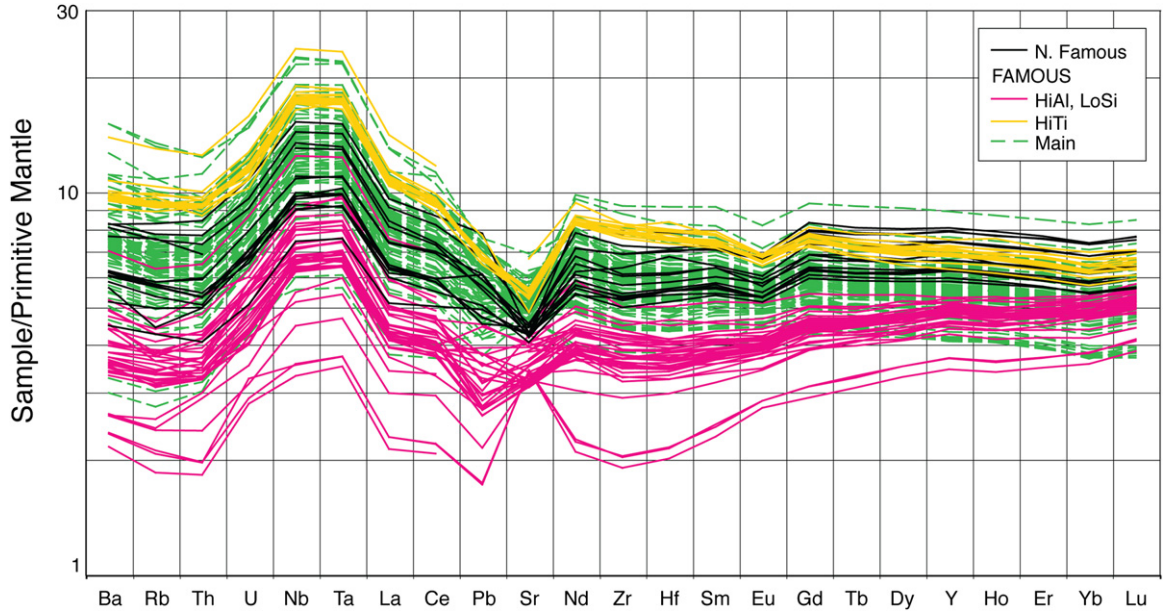

Fig. 3. Primitive mantle-normalized spidergrams (Sun and McDonough, 1989) showing the trace element patterns of the main compositional groups from both segments. Note the downward sloping patterns from Lu to Sm of the HiAl–LoSi group that cross over the patterns from the Main group. HiTi lavas have elevated trace element concentrations. Three HiAl–LoSi lavas from near the northern fracture zone at FAMOUS are significantly more depleted and have positive Sr anomalies (see text).

A few samples from both the Main and HiAl–LoSi lavas have higher Ba concentrations, leading to relatively high Ba/La ratios, which can be observed as Ba spikes on primitive mantle normalized trace element spidergrams. The HiTi lavas identified from major elements are marked by higher overall abundances of most trace elements, in correspondence with their high TiO_2 contents.

The N. Famous samples are some of the most depleted lavas in the dataset in terms of moderately incompatible trace element ratios and 90-values. Despite lower moderately incompatible ratios than the Main FAMOUS lavas (e.g., Zr/Y), they have nearly identical highly incompatible trace element ratios (e.g., Th/La). The N. Famous lavas extend to La/Sm ratios as low as the depleted HiAl–LoSi FAMOUS samples, but they have 90-value concentrations higher than the HiAl–LoSi lavas and do not possess the low Dy/Yb ratios.

A characteristic of all lavas from this region emerging from these observations is the elevated highly incompatible trace element ratios such as Th/La, Nb/La and Ba/La, coupled with only modestly enriched moderately incompatible element ratios. The highly incompatible element ratios are as high or higher than those of the most Azores plume-influenced ridge segments (KP-2 and -3) far to the north (Gale et al., 2011), even though their moderately incompatible element ratios (e.g., Zr/Y, Sm/Yb) are much lower.

3.3. Isotopes

The new isotope data indicate mantle heterogeneity within each of the two studied segments (Fig. 4), as noted for FAMOUS by le Roex et al. (1996). Pb isotopes vary considerably from $^{206}Pb/^{204}Pb < 18.5$ to > 19.0. $^{143}Nd/^{144}Nd$ in FAMOUS lavas varies from 0.513064 to 0.513133, but N. Famous lavas extend this range up to 0.5132. Sr isotopes vary outside analytical error, but for the FAMOUS region do not correlate well with other isotope systems, particularly Pb (see Fig. S4 in Supplementary material). There is a good correlation between Sr and Pb for N. Famous, with the exception of one analysis from Dosso et al. (1999). Nd and Pb isotopes correlate very well with one another, with the exception of one analysis from Frey et al. (1993).

The Main group encompasses the full isotopic range at FAMOUS. The most enriched E-MORB sample is more enriched isotopically than many samples seen at the LS segment farther north. The HiAl–LoSi group occupies the middle of the FAMOUS array and is not distinct isotopically. The HiTi lavas are also clustered in the middle of the array. Substantial isotopic variations occur within the N. Famous segment despite the small number of sample locations and its short length.

The poor correlations of the $^{87}Sr/^{86}Sr$ data at FAMOUS raise the question of whether the $^{87}Sr/^{86}Sr$ may have been influenced by seawater. Fresh, unaltered glasses were handpicked and leached prior to dissolution, making it unlikely that the seawater signal is caused by surface alteration. Instead, a seawater effect could be produced by direct interaction with the magma or assimilation of some altered material (e.g., Michael et al., 1989; Schiffman et al., 2010). This possibility could be explored in future work with chemical proxies for seawater such as Cl^-. Due to the uncertainties associated with the $^{87}Sr/^{86}Sr$ data, interpretation for the remainder of this paper will be based upon Nd and Pb isotopes only.

In a broader context, the FAMOUS and N. Famous lavas are isotopically intermediate between a representative depleted MORB mantle (DMM) and the fields of the Azores islands. The N. Famous samples, despite being geographically situated between the FAMOUS and LS segments, are not intermediate isotopically but instead extend the depleted end of the FAMOUS array in both Pb and Nd isotopes. Even with all the major and trace element variability, the samples from FAMOUS and N. Famous form a tight linear trend in the Pb–Pb diagram pointing toward lavas from the Azores ridge segments (KP-2 and -3) and islands (Fig. 4a), suggesting the source of isotopic enrichment is related to the Azores plume. The subtle slope difference between the FAMOUS and N. Famous trends, however, likely indicates a

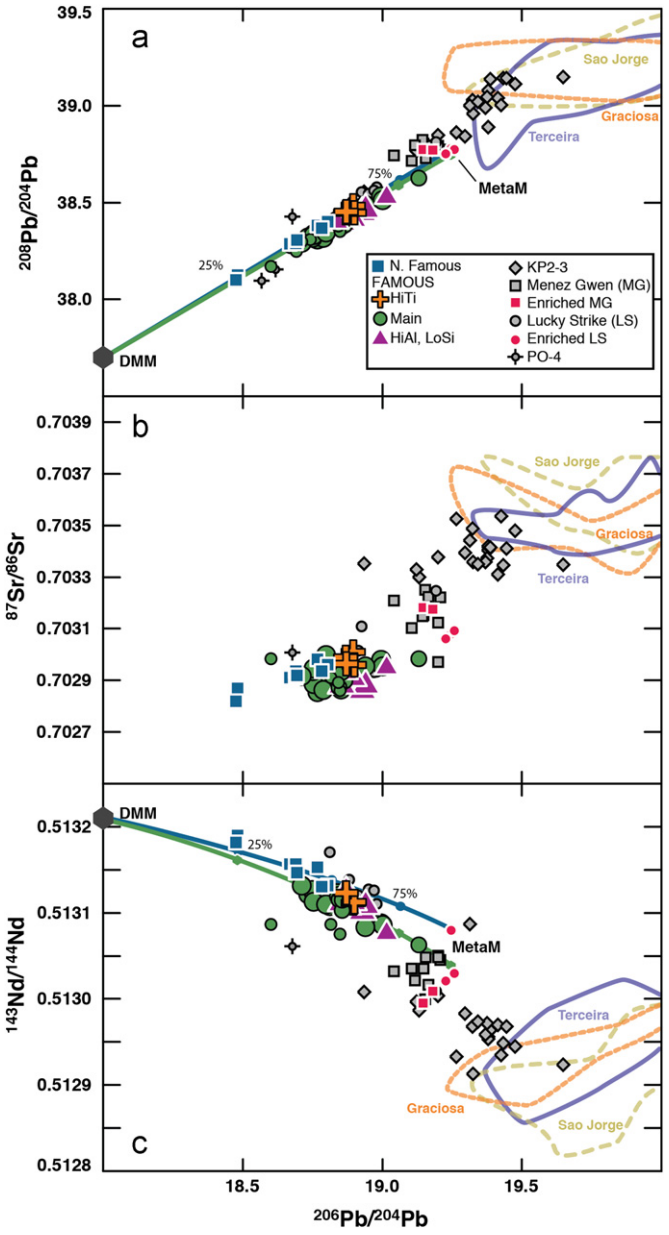

Fig. 4. (a–c) $^{208}Pb/^{204}Pb$, $^{87}Sr/^{86}Sr$ and $^{143}Nd/^{144}Nd$ vs. $^{206}Pb/^{204}Pb$. Data from this study and others (Agranier et al., 2005; Chauvel and Blichert-Toft, 2001; Dosso et al., 1999; Frey et al., 1993; Gale et al., 2011; Ito et al., 1987; Yu et al., 1997). Fields are also shown for the islands of Terceira, Sao Jorge and Graciosa (data taken from GeoROC). Isotope data from before 1985 is not shown in the figures. For consistency, all data were renormalized according to the normalization scheme given in the Supplementary material. For FAMOUS, smaller symbols indicate published data. All FAMOUS and N. Famous samples are intermediate in composition between depleted mantle (DMM) and the Azores. Within this general enrichment, however, N. Famous samples are on the depleted end of the array. This is unexpected given that N. Famous is geographically closer to the Azores. Note also the complete overlap between transitional LS samples (gray circles) and Main FAMOUS samples. There is a strong correlation between $^{143}Nd/^{144}Nd$ and $^{206}Pb/^{204}Pb$, but only weak correlation in the FAMOUS $^{87}Sr/^{86}Sr$ with $^{206}Pb/^{204}Pb$. Shown are mixing curves between DMM and MetaM (the metasomatized mantle source, Supplementary Table S7) for FAMOUS (green line) and N. Famous (blue line). (For interpretation of the references to color in this figure legend, the reader is referred to the web version of this article.)

small difference in the isotopic composition of the enriched end member. This is not surprising given the extensive isotopic variability seen in Azores plume basalts.

A noteworthy observation comes from comparison of the trace element and isotopic data. All chemical groups at FAMOUS and N. Famous are less enriched isotopically than KP-2 and -3 (Azores MORB) samples, and yet as discussed above they have as high or higher highly incompatible trace element ratios. This characteristic is similar to (but less extreme than) the feature displayed by the E-MORB seen at the nearby LS and MG segments (Gale et al., 2011).

The substantial isotopic variability found in the present study marks a major change in the fundamental constraints on the interpretation of data from this region. Sr isotope studies in the 1970s (White and Schilling, 1978) indicated a homogeneous radiogenic isotope composition for the FAMOUS segment, which led to the presumption of a homogeneous source and all trace element variations produced by melting processes (e.g., White and Bryan, 1977; Langmuir et al., 1977). The present data show clearly that source heterogeneity is substantial within both the FAMOUS and N. Famous segments.

The question is then to what extent the trace element variations are controlled by the source variations indicated by the isotopes. Fig. 5 compares the Pb isotope variations with three trace element ratios reflecting a range of incompatibility—Th/La, La/Sm and Zr/Y. The correlations for N. Famous, Main and HiTi samples suggest a major portion of the chemical variations is produced by source heterogeneity. In contrast, the HiAl–LoSi lavas are noticeably offset from these correlations to more depleted values of all ratios, including Th/La. HiAl–LoSi samples appear to have been influenced by recent events that have fractionated the trace element ratios.

Two other observations from Fig. 5 are significant. First, the variation in trace element ratios at a single isotopic composition remains substantial (e.g., $>25\%$ for both Zr/Y and La/Sm). This suggests that variations in extent of melting of the various source compositions are also occurring. Second, on the Th/La–$^{206}Pb/^{204}Pb$ diagram the data array for samples from this region does not trend toward the composition of the segments nearest the Azores Islands (KP-2 and KP-3), indicating that mixing of plume melts or sources with a depleted end member cannot be the primary explanation for the FAMOUS and N. Famous data.

3.4. Complexities of the regional gradient

The data shed light on the detailed characteristics of the regional gradient in enrichment toward the Azores platform, seen in Fig. 6. For consistency with the gradient, N. Famous lavas would be more enriched than the FAMOUS lavas, as N. Famous is closer to the Azores. Yet the N. Famous samples are less enriched in their trace element and isotopic signature than FAMOUS samples. Furthermore, in terms of both isotopes and Th/La ratios, the FAMOUS lavas have similar ranges to the LS segment to the north, with the exception of the subset of enriched samples from the LS segment center (Gale et al., 2011). Clearly, the regional gradient is not smooth and continuous, and cannot reflect simple source mixing between a depleted mantle (with Th/La ~ 0.06) and an enriched source associated with the Azores plume (see also Gale et al., 2011).

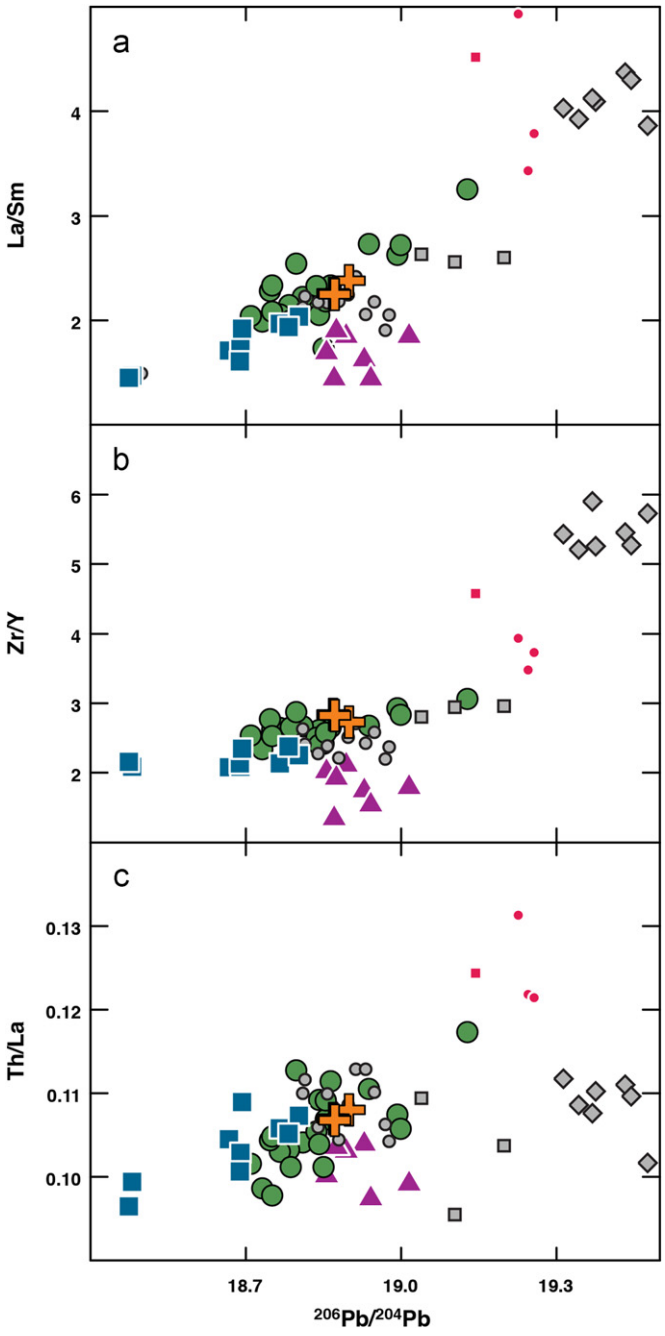

Fig. 5. (a–c) La/Sm, Zr/Y and Th/La vs. $^{206}Pb/^{204}Pb$ for N. Famous and FAMOUS basalts. Smaller symbols indicate published data (references as in previous figures). E-Melts from the Lucky Strike segment are shown as small red symbols. Samples from the KP-2 and KP-3 segments closest to the Azores hot spot are gray diamonds. Note the remarkably coherent relationship between incompatible trace element ratios and $^{206}Pb/^{204}Pb$ seen in all but the HiAl–LoSi group from FAMOUS. The pronounced offset of HiAl-LoSi lavas is evidence that a recent melting process has disrupted their trace element composition. Note in (c) that the N. Famous and FAMOUS data cannot be explained by mixing between depleted mantle and the KP-2 and KP-3 segments. (For interpretation of the references to color in this figure legend, the reader is referred to the web version of this article.)

4. Discussion

The observations raise four questions that need to be addressed: (1) the cause of the variations in source for the FAMOUS and N. Famous segments; (2) how source and melting variations interact to produce the spectrum of lava compositions; (3) the cause and implications of the contrast between isotopic and trace element gradients south of the Azores (see Fig. 6); and (4) the origin of the HiAl–LoSi lavas.

4.1. Source and melting variations

The linear trends of the principal component of the data in most trace element diagrams (excluding the HiAl–LoSi lavas), and

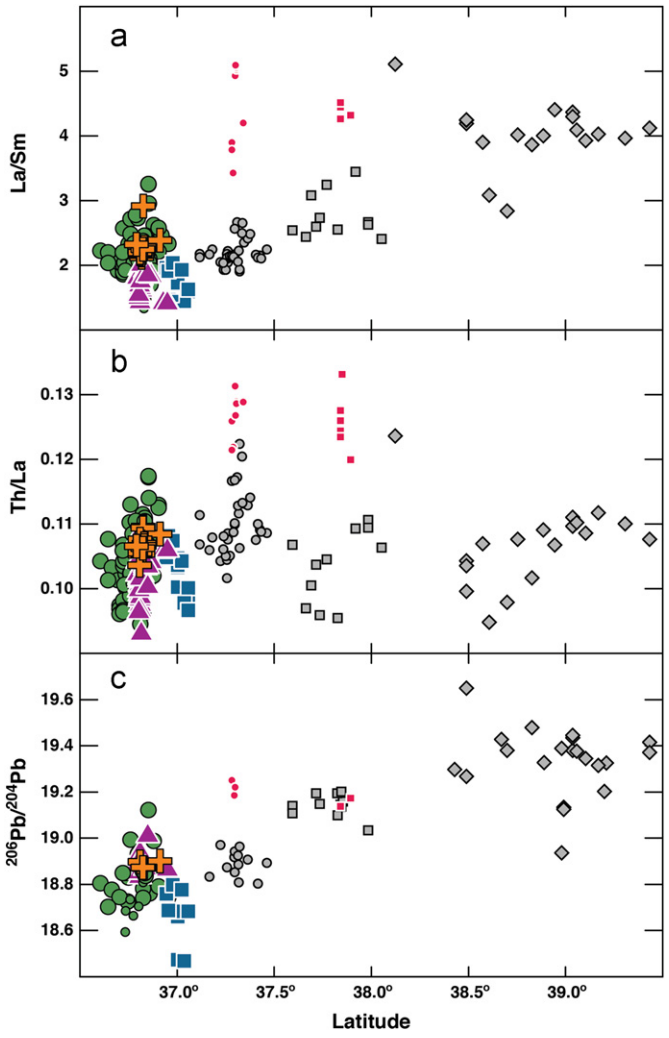

Fig. 6. (a–c) La/Sm, Th/La and $^{206}Pb/^{204}Pb$ vs. latitude for a portion of the MAR south of the Azores. Data from this study and other sources previously cited. Symbols are as in Fig. 4; errors on the ratios are smaller than the symbols. Note the rich complexity of the geochemical gradient. Pb isotopes show the most systematic decrease with latitude, but N. Famous is more depleted than segments to both north and south. While the baseline La/Sm tends to decrease southward, Th/La shows almost no change (or even increases) from the Azores platform lavas south to FAMOUS. N. Famous in particular has anomalously high Th/La ratios given such low La/Sm and $^{206}Pb/^{204}Pb$ values. This feature of the data is strongly suggestive of the metasomatized source as the enriched mixing component giving rise to the gradient. The metasomatized source strongly influences highly incompatible trace element ratios (see the highly enriched E-Melts from LS and MG) without a large effect on isotopes and moderately incompatible element ratios.

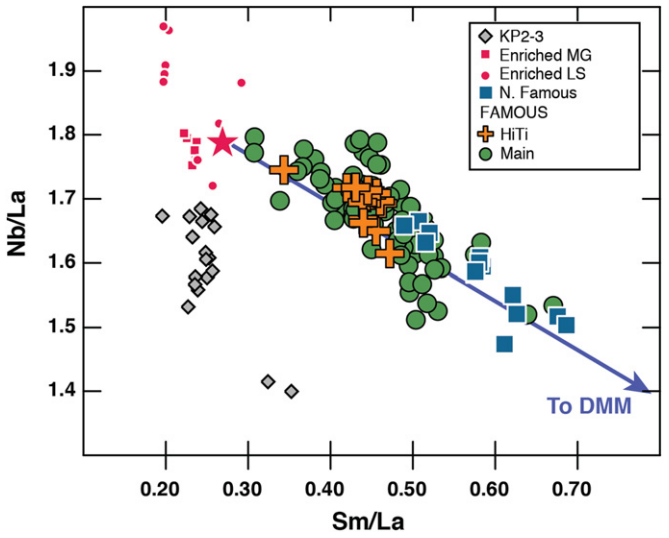

Fig. 7. Nb/La vs. Sm/La of basalts from N. Famous, FAMOUS, KP2-3 and E-Melts from Lucky Strike (LS) and Menez Gwen (MG). E-Melts from LS and MG have much higher highly incompatible trace element ratios than Azores platform lavas (KP2-3) for a given Sm/La. All samples from FAMOUS and N. Famous appear to be mixing toward this E-Melt type component (indicated by the red star) rather than toward the more "plume-like" component represented by the KP2-3 lavas. This explains how the FAMOUS and N. Famous samples could have Th/La and Nb/La similar to the Azores platform lavas while being much less enriched in incompatible trace element concentrations and isotopes (see Fig. 5). Shown is a mixing curve between 10% melts of DMM and MetaM for comparison. (For interpretation of the references to color in this figure legend, the reader is referred to the web version of this article.)

the linear isotopic arrays, strongly suggest mixing between two end members to control the source variations. Fig. 5c shows that the melts from the ridge segments most influenced by the Azores plume are not a suitable enriched end member. What then is the end member? Inspection of Fig. 5c shows that the enriched melts from LS (Gale et al., 2011) are close to a projected end of a potential mixing array of the FAMOUS and N. Famous lavas. This can be better evaluated graphically on diagrams with common denominators such as Fig. 7. On this plot of Nb/La vs. Sm/La, the samples form a linear mixing trend that extends toward the highly enriched melts (E-Melts) seen at nearby segment LS (red star on figures). The E-Melts at LS have higher incompatible trace element ratios than the Azores platform melts for a given Sm/La, and can be explained by a low-degree melt of the Azores plume source that serves to metasomatize the source of the E-Melts (Gale et al., 2011). The mixing trends of the FAMOUS and N. Famous data imply that this E-Melt type component, rather than a pure Azores plume component, is the appropriate enriched end member.

These mixing trajectories must be mixing of sources rather than of magmas, because mixing of magmas would lead to linear data arrays on plots of trace element abundances in lavas corrected to be in equilibrium with Fo_{90} olivine, which is not observed. Fig. 8a shows a plot of Yb_{90} vs. Nb_{90}. Yb is less sensitive to source variability and more sensitive to extent of melting (F) variations. Nb, a highly incompatible element, is more sensitive to source variations. The variations in both parameters suggest that variations in extent of melting (F) and mantle source are important. The importance of F variations has been emphasized in earlier studies of FAMOUS lavas (Frey et al., 1993; Langmuir et al., 1977; le Roex et al., 1996).

To test this model quantitatively (see Supplementary material for full details) we used the 33 samples from FAMOUS and N. Famous that have both trace element and isotopic measurements (not including HiAl–LoSi samples—see discussion). We first corrected the raw trace element data back to 8.6% MgO (Langmuir et al., 1992) and then added olivine to achieve equilibrium with Fo_{90} olivine to have "primary" melts to compare with model output. The model simply (a) mixes two mantle sources (depleted and enriched) in varying proportions and then (b) melts that mixed source.

The enriched source is a metasomatized source from LS (Gale et al., 2011) but with slightly lower (20%) Ba, Rb and Cs abundances since mixing trajectories show the LS E-melt is slightly high in these elements. The selected metasomatized source from LS was the most appropriate enriched end member for the FAMOUS and N. Famous data array (Fig. 7). The high Ba/La, Rb/La and Cs/La (and not Th/La or Nb/La) of LS E-Melts suggest that modest amounts of phlogopite might have influenced the generation of the mantle sources for these lavas (e.g., Green et al., 2000). The depleted source is the DMM published by Salters and Stracke (2004), with slight adjustments to Y, Zr, Nb and Pb within

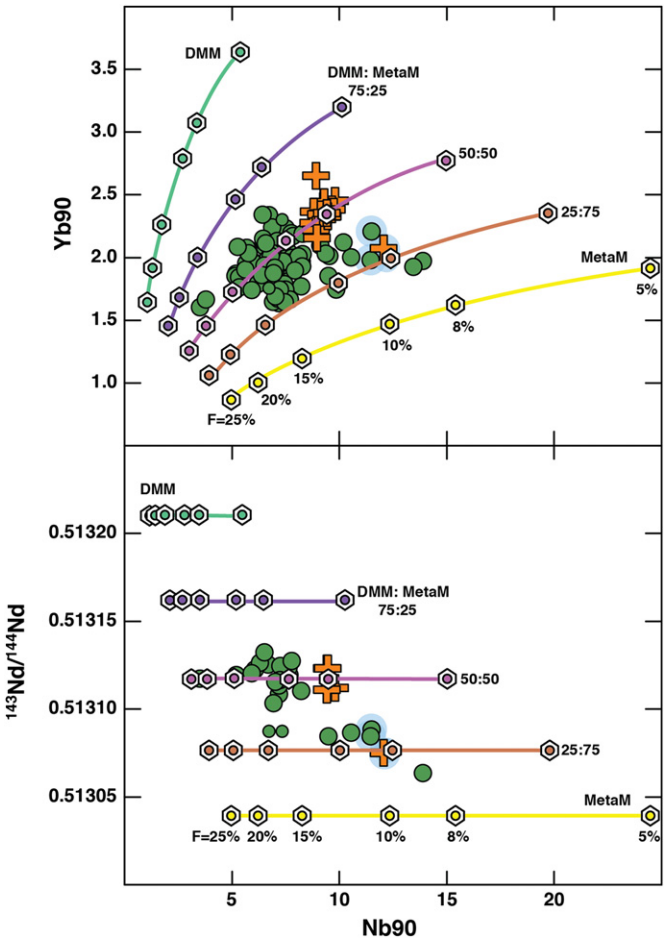

Fig. 8. (a and b) Yb_{90} and $^{143}Nd/^{144}Nd$ vs. Nb_{90} of FAMOUS lavas (not including the HiAl–LoSi samples which have a separate petrogenesis—see text). Symbols as in previous figures. Five sources that are mixtures between a metasomatized enriched source (Gale et al., 2011) and a DMM (Salters and Stracke, 2004) are shown (different colored lines). These sources are then melted to various extents (5–25%, demarcated by hexagons). The grid shows the combined effects of *F* and source composition on lava compositions. This simple model is able to account well for the trace element and isotopic variability of FAMOUS basalts through a combination of *F* and source variation. The combination that works for a given sample in trace element diagrams also holds when considering isotopic compositions (see highlighted samples). (For interpretation of the references to color in this figure legend, the reader is referred to the web version of this article.)

their reported error (Table S7). Due to the subtle offset of N. Famous lavas in $^{208}Pb/^{204}Pb$ vs. $^{206}Pb/^{204}Pb$, we use different Pb and Nd isotopic compositions for the metasomatized sources at N. Famous and FAMOUS (Table S7). This is reasonable given that isotopic variability exists within the E-Melts from LS and MG (Gale et al., 2011). The isotopic composition of the DMM end member is estimated to be at the convergence of the FAMOUS and N. Famous trends.

For each sample, differences between model output and primary magma compositions for trace elements and isotopes were minimized by varying the proportion of metasomatized mantle in the source and the extent of melting (*F*). The melting of the mixed sources was modeled as non-modal batch melting without garnet in the residue (see Table S7 for mantle source compositions, partition coefficient (*D*) values, mineral modes and melting reactions). Despite the simplicity of this model, all 20 incompatible trace element contents are fit to better than 10% with few exceptions (Pb worse in 8 cases: avg. misfit in these cases is 13.5%, max. misfit of 19.6%; U worse in 7 cases: avg. misfit in these cases is 13.6%, max misfit of 16.7%). Also, all $^{143}Nd/^{144}Nd$ and $^{207}Pb/^{204}Pb$ and most $^{206}Pb/^{204}Pb$ and $^{208}Pb/^{204}Pb$ compositions were fit within typical analytical error, with only 10 samples slightly worse in $^{206}Pb/^{204}Pb$.

The results require a large proportion of metasomatized mantle in the source of FAMOUS lavas (43–82%), with an average of 55%. *F* varies from 7.6% to 13.4% with an average of 10.3%. At N. Famous, the proportion of metasomatized mantle in the source ranges from 25% to 47%, with a mean of 37%, and *F* ranges from 10.4% to 13.9% with an average of 12.6%.

Given the simplicity of the model, it is remarkable that the disparate groups seen at the FAMOUS segment are all accounted for, including Main samples with both high and low Ba contents, and HiTi samples. The HiTi group, which based on major elements alone required a different parental magma, can be explained through lower extents of melting of a moderately enriched source. Low extents of melting are also consistent with their low CaO contents, as CaO contents in primary magmas decrease as extent of melting decreases when clinopyroxene is present in the residue (e.g., Jaques and Green, 1980; Longhi, 2002).

Another intriguing outcome of the model is a correlation between extent of melting and quantity of metasomatized source (Fig. 9). One might expect that the metasomatized source, with its higher volatile contents, would melt more. Instead, the modeled *F* decreases as the quantity of enriched, metasomatized source increases. This cannot be the effect modeled by Asimow and Langmuir (2003), because their models considered constant mantle source water contents within an entire melting regime, not two different mantle components with different water contents within a single melting regime.

How could the extents of melting be less when a more hydrous mantle begins melting at lower temperatures or greater depths than a dry mantle? A possible explanation emerges from consideration of the geometry of the melting regime, based on the melting triangle and "residual mantle column" concepts presented by Langmuir et al. (1992). At the edges of the melting regime, where extents of melting are small, the more hydrous (likely to melt) component is the dominant component. So lower extents of melting of enriched sources are found in the "wings" of the melting regime, and may rise and flow along high-porosity channels to erupt at the top of the melting regime (e.g., Hebert

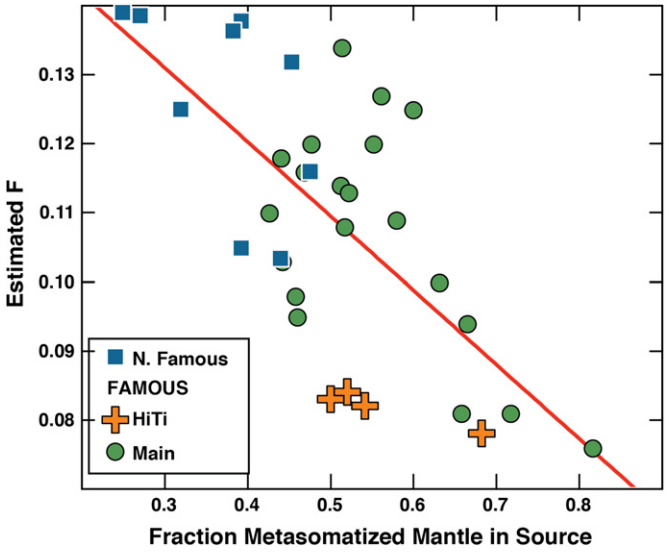

Fig. 9. Estimated *F* vs. fraction metasomatized mantle in source for modeled lavas from N. Famous and FAMOUS. Shown is a least-squares regression through the data. To the first order, there is a negative correlation between the fraction of metasomatized mantle in the source and the extent of melting. See discussion (Section 4) in text.

and Montési, 2010; Katz, 2008; Sparks and Parmentier, 1991). This would provide a mechanism for low-degree melts of an enriched component to be one end member of the *F* vs. source correlation. Another contributing factor to the relationship of *F* and source may be the more refractory nature of the metasomatized source in terms of major element composition (higher Mg#; Gale et al., 2011), which would limit its total fusibility.

N. Famous is both more depleted and has a higher mean extent of melting than FAMOUS. One possible explanation is that the N. Famous segment is so short that it is does not sample as effectively the wings of the melting regime that deliver the enriched component. This would lead to a higher mean extent of melting and a less enriched source composition.

The correlation between extent of melting and source depends on the metasomatized source composition modeled by Gale et al. (2011) for LS E-Melts. Specific major element characteristics of these E-Melts (e.g., high Al, low Si) led the authors to the conclusion that they are ~7% melts. Gale et al. (2011) inverted for the source trace element composition of these E-Melts assuming an *F* of 7%. The modeled source composition, then, is dependent upon this choice of *F*. Despite these uncertainties, however, there is strong evidence for the *F* choice made by Gale et al. (2011) for the LS E-Melts. The inferred relationship between *F* and quantity of metasomatized source is intriguing, but involves a significant chain of reasoning.

4.2. Origin of the HiAl–LoSi lavas

The HiAl–LoSi lavas have similar isotopic composition to other samples from this region, but a distinctive trace element signature that combines comparable highly incompatible element ratios with very low incompatible element abundances and distinctively low Dy/Yb. Olivine-hosted melt inclusions with similar but more extreme signatures have been found in these lavas (Laubier et al., 2012). The melt inclusions have SiO_2 contents as low as 46.6%, Al_2O_3 as high as 18.4 wt%, a strong depletion in the most incompatible elements and similarly low Dy/Yb. Laubier et al. (2012) argue that such ultra-depleted melt inclusion compositions require a source modified by previous melt removal. The melt removal must occur in the garnet stability field to retain Yb, which is compatible in garnet, and produce a source with low Dy/Yb. Subsequent melting of this residue without garnet present would generate depleted, low Dy/Yb melts.

Many of the melt inclusions, however, are far more depleted in the most incompatible elements, leading to subparallel trace element patterns between HiAl–LoSi melt inclusions and lavas only in the elements Gd through Lu. The HiAl–LoSi lavas are instead subparallel to the Main lavas in highly incompatible elements. The HiAl–LoSi lavas are also intermediate in major and trace element concentrations (e.g., avg. SiO_2 49 wt%, Al_2O_3 16.2 wt%, La 3.1 ppm) between Main lavas (51%, 14.9%, 5.8 ppm) and HiAl melt inclusions (~47%, ~17.5%, 0.59 ppm).

These features can be explained by a magma mixing model. Mixing a typical HiAl melt inclusion with the average Main lava in a 50:50 proportion fits every major and trace element in the average HiAl–LoSi basalt to better than 6%, with P the only exception (fit to 12%; details given in Supplementary material see mixing curves in Fig. 2). The HiAl–LoSi lavas receive their "depleted" low Dy/Yb signature from the HiAl melt inclusions, and their "enriched" incompatible element signature from the Main lavas.

Two other lines of evidence support a mixing model. First, there is a high Ba signature present in some HiAl–LoSi lavas. This could be puzzling because high Ba is an enriched signature, and low Dy/Yb a depleted signature. As Main lavas include both high and low Ba samples, mixing with diverse Main lavas could lead to both high and low Ba mixtures. Second, olivines within the HiAl–LoSi lavas contain melt inclusions of both HiAl and "Main" compositional types, consistent with both melts being present (and mixing) to form the HiAl–LoSi lavas (Laubier et al., 2012).

Three HiAl–LoSi glasses found near the northern fracture zone (ARP74-14-31,32,33) have unique characteristics, including Sr anomalies ($Sr/Sr^* = [Sr_N/sqrt(Ce_N * Nd_N)]$) of 1.5–1.61, high Ba/La and the most depleted compositions of any lavas from the FAMOUS segment (Fig. 3). Positive Sr anomalies have also been found in certain HiAl melt inclusions from FAMOUS (Laubier et al., 2012), and were used as evidence for assimilation of plagioclase-rich cumulates in the crust. Such assimilation is a mechanism for generating the high Sr and high Ba seen in these melts. The coupling of depleted trace element signatures with Sr anomalies has been emphasized in the literature (e.g., Danyushevsky et al., 2004, 2003; Gurenko and Sobolev, 2006; Kamenetsky and Crawford, 1998; Slater et al., 2001; Sobolev et al., 2000), but largely with regard to melt inclusions. The FAMOUS segment shows such compositions in both melt inclusions and lavas.

These interpretations differ from the explanation of Langmuir et al. (1977) for the origin of the low Dy/Yb samples by dynamic melting where fractional melting with some melt retained in the residue begins in the garnet field. Dynamic melting adequately accounts for the trace element characteristics of these samples as well as their similar isotopic composition to the Main lavas. It does not account for the major elements, however. For the dynamic melting model, the low Dy/Yb lavas would be the final product from the top of the melting regime, and hence would be expected to have higher SiO_2 than other lavas. Instead, these lavas have the lowest SiO_2. The model of an earlier depletion event and late stage magma mixing is able to account for both major element and trace element constraints.

4.3. Implications for the regional gradient near the Azores plume

The classical model for gradients around plumes involves mixing between DMM and a plume source, with plume mantle progressively diluted as it disperses along the ridge axis (e.g., Dosso et al., 1999; Schilling, 1975; Schilling et al., 1983). A more recent model considers the mantle a mixture of depleted and enriched components, with no compositional difference between plumes and ambient upper mantle (Ingle et al., 2010; Ito and Mahoney, 2005a, 2005b). The different components melt at different depths depending on their fusibility, so changes in mantle flow can lead to variations in the rate at which these components melt. These authors argue that the most pronounced signature of the enriched components is in lavas nearest the plume where deep mantle flow is the strongest. Fast mantle flow at depth, where the enriched veins begin melting, enables a larger contribution of the enriched component. The geochemical gradient is created by variable mantle flow with distance from the plume, rather than variable mantle composition.

Neither the variable composition nor the variable flow models accounts for the data from the ridge segments south of the Azores. Both models predict that highly incompatible trace element ratios and radiogenic isotope enrichment should decrease systematically with distance from the most plume-influenced segments. This is not the case for segments south of the Azores platform.

Instead the data can be explained by creation of a metasomatized source from low-degree melts of the Azores plume. This metasomatized source is "plume-like" in that it has very similar isotopic characteristics to the Azores, but it has somewhat reduced trace element concentrations and elevated highly incompatible trace element ratios. The necessity for a metasomatic component instead of bulk plume material is particularly evident for N. Famous lava compositions, which have Nb/La and Th/La as

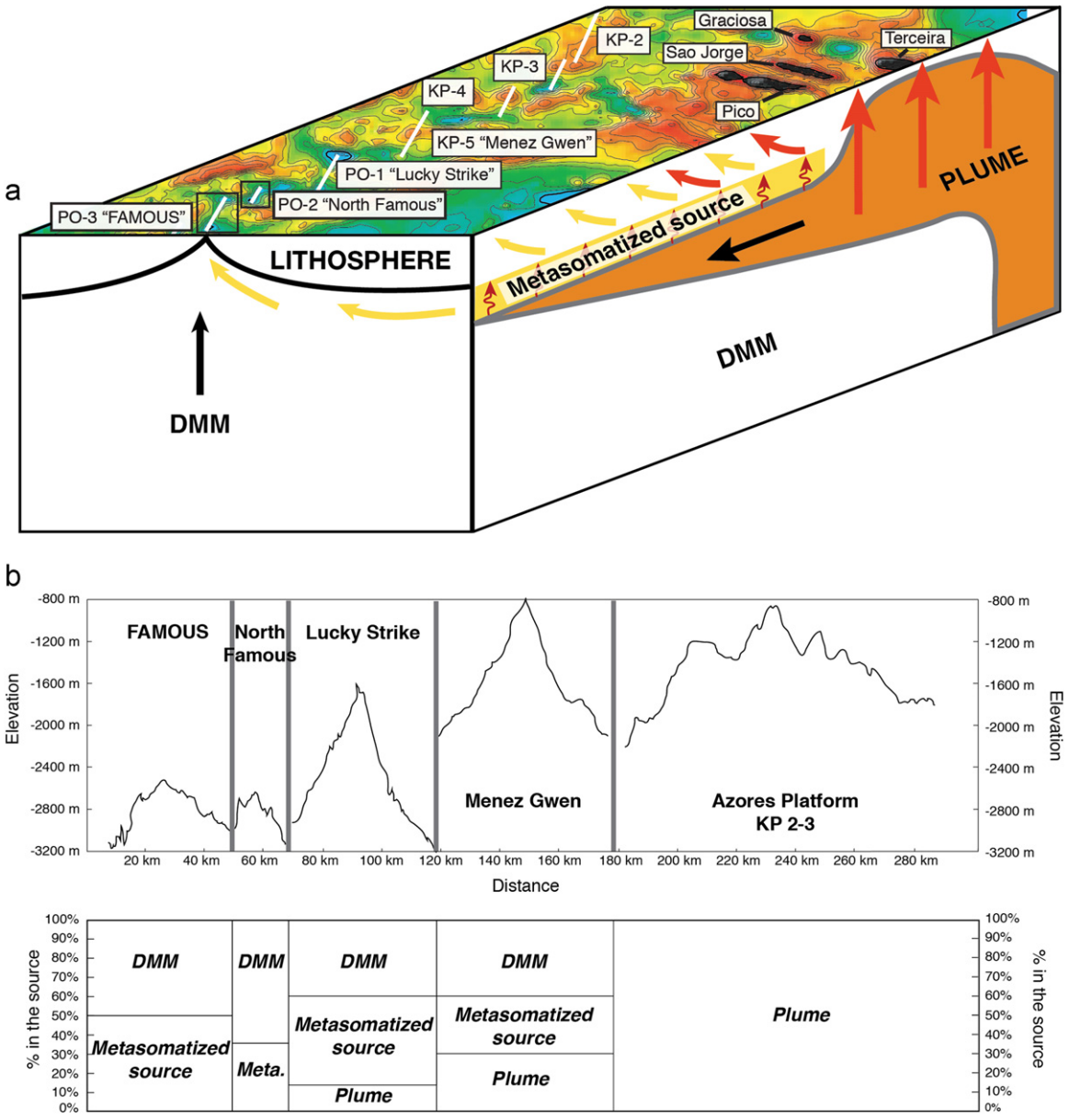

Fig. 10. Cartoon illustrating (a) our conceptual model of melting and mixing processes occurring near the ridge and (b) the average proportions of components that contribute to the sources of the various ridge segments. (a) In this model, plume material upwelling near the island of Terceira is deflected to the southwest (the direction of upper mantle shear flow). MetaM is generated east of the ridge through a mixture of a slightly refractory DMM and a low-degree melt of the Azores plume; these low-degree melts of the plume are injected into the overlying depleted lithospheric mantle, creating MetaM (see text for details). The presence of hot plume material near the depleted lithospheric mantle, coupled with the addition of water from the low-*F* melt, might permit the remobilization of this lithospheric mantle by decreasing its viscosity. MetaM would then flow as part of the asthenosphere toward the different ridge segments, where it mixes with ambient DMM. The contributions of each component (plume, MetaM and DMM) to the source of the lavas vary along the ridge. They are represented by arrows showing that the plume component is present only at KP2-3, Menez Gwen and Lucky Strike, and the fraction of MetaM decreases from Menez Gwen to FAMOUS (with the exception of N. Famous, even more depleted). (b) The proportions of the different source components, taken as average proportions for each segment, reflect the inferred changes in source composition along the ridge. (1) The enriched end member changes from being the Azores plume at KP2-3 to MetaM near LS, with MG having enriched contributions from both plume and MetaM. (2) The depleted end member reflects mixing between DMM and small amounts of Azores plume, with the Azores plume contribution dying out between LS and N. Famous.

high as the Azores platform lavas, despite far less enriched La/Sm, trace element concentrations and isotopic signatures (Figs. 6 and 7). There must be a means to drive up the highly incompatible trace element ratios in the N. Famous lavas without over-enriching their La/Sm and trace element concentrations. Such a mechanism is addition of very low-degree melts to create a metasomatized source that mixes with DMM to produce the diversity of sources observed.

There is also the question of the depleted end member. Gale et al. (2011) showed that for the LS segment, the metasomatized source mixed with a background mantle that was a mixture of the Azores plume source and DMM, with the proportion of plume in the LS depleted end member being very low. For FAMOUS and N. Famous, the mixing trajectories point toward DMM itself, rather than to a mixture of DMM with the Azores plume. The systematics of the data then suggest that the enriched end member changes from being the Azores plume in the north to a source metasomatized by a low-degree melt from the plume. The depleted end member reflects mixing between DMM and small amounts of Azores plume, with the Azores plume contribution dying out between LS and N. Famous.

A challenge is to frame a physical model consistent with the geochemical constraints. The model needs to generate a metasomatized source through a mixture of a slightly refractory DMM (~4% melt removed) and a low-degree melt of the Azores plume (Gale et al., 2011). How might these two components combine? Yang et al. (2006) showed that plume material upwelling near the island of Terceira is deflected to the southwest (the direction of upper mantle shear flow). Meanwhile, mantle melting at the nearby spreading ridges creates a slightly refractory mantle, which flows eastward (and westward), perpendicular to segment axes. Such shallow, eastward-flowing, slightly refractory mantle intersects and overlies the southwestward flowing plume material. Low-degree melts of the plume could then be injected into this depleted lithospheric mantle, creating the metasomatized source. The proximity of depleted lithospheric mantle to hot plume material, coupled with the addition of water from the low-*F* melt, might remobilize the lithospheric mantle by decreasing its viscosity. Water especially has been shown to strongly affect mantle viscosity (Hirth and Kohlstedt, 1996). The remobilized, metasomatized mantle would then flow as part of the asthenosphere toward MG, LS, N. Famous and FAMOUS, where it mixes with ambient DMM and gives rise to the geochemistry of the lavas. A cartoon illustrating this conceptual model with the average proportions of components that contribute to the sources of the various ridge segments is shown in Fig. 10.

A question is whether the model of low-*F* melts creating the geochemical gradient seen in MORB south of the Azores applies to other plumes. In recent data from the Galapagos spreading center (Ingle et al., 2010), E-MORB with higher highly incompatible trace element ratios than the plume MORB are not found. Still, trace element ratios like Nb/La and Ba/La remain as high as the isotopically enriched plume MORB for more than 200 km, whereas more moderately incompatible trace element ratios like Zr/Y and Sm/Yb decrease immediately (within 50 km) away from the plume. Elevated highly incompatible trace element ratios coupled with lower moderately incompatible trace element ratios, seen in the Galapagos, are the very characteristics possessed by the T-MORB near the Azores. Two areas of future exploration will include the extent to which the low-F model applies to plume-ridge interactions globally, and the problem of three-dimensional mantle flow and melting during plume-ridge interaction.

5. Conclusions

The main conclusions of this study can be summarized as follows:

1. FAMOUS lavas show significant diversity within a single segment, indicating multiple supply of magmas along the length of the segment, and the ability of melting processes to deliver highly diverse melts over short distances and times.
2. A successful model for FAMOUS and N. Famous basalts involves variable degrees of melting of a two-component source. HiAl–LoSi lavas are an exception to this model, and are generated by mixing between Main FAMOUS lavas and a highly depleted composition present in some melt inclusions from this region (Laubier et al., 2012).
3. The enrichment signal in this region is not simply created by mixing with an Azores plume source. Instead, the enriched source is generated by adding deep, low-degree melts of Azores plume material to a mantle depleted by a small amount of previous melt removal (Gale et al., 2011). Our model involving mixing between this metasomatized mantle and a depleted mantle applies to multiple segments in this region.
4. The regional gradient in geochemistry is not systematic with distance from the Azores. The very short N. FAMOUS segment is closer to the Azores and yet its lavas are more depleted in trace element ratios and isotopes than FAMOUS lavas. This suggests that the delivery of the enriched component to individual segments may be influenced by segment size.

Acknowledgments

Thanks to Michael Jercinovic at UMass Amherst for assistance with the electron microprobe, to Zhongxing Chen for his support with the ICP-MS at Harvard, to Juraj Farkas for his assistance with the TIMS at Harvard and to Jurek Blusztajn for his help with the Neptune at WHOI. We appreciate the FAMOUS samples provided by René Kerbrat at IFREMER, Brest, by Jim Broda at the WHOI Sea Floor Samples Laboratory and by Leslie Hale of the Smithsonian Institution. Earlier work on some of the samples in this study also had contributions from Kerstin Lehnert, Terry Plank, Dana Desonie, Yaoling Niu and Paul Asimow. This manuscript greatly benefited from reviews from two anonymous reviewers, and from the editorial support by Tim Elliott. This work was supported by the NSF Grant OCE-9103548 to C.H. Langmuir at Lamont-Doherty Earth Observatory and OCE-0752281 and OCE-1061264 at the Harvard University.

Appendix A. Supporting information

Supplementary data associated with this article can be found in the online version at http://dx.doi.org/10.1016/j.epsl.2013.01.022.

References

Agranier, A., et al., 2005. The spectra of isotopic heterogeneities along the mid-Atlantic Ridge. Earth Planet. Sci. Lett. 238 (1–2), 96–109.
Asimow, P.D., Langmuir, C.H., 2003. The importance of water to oceanic mantle melting regimes. Nature 421, 815–820.
Ballard, R.D., et al., 1975. Manned submersible observations in Famous area—Mid-Atlantic Ridge. Science 190 (4210), 103–108.
Bézos, A., Escrig, S., Langmuir, C.H. Empirical calibration of olivine, plagioclase and clinopyroxene mineral-melt partition coefficients in presence of water: an improved fractionation model, in preparation.
Bougault, H., Hékinian, R., 1974. Rift valley in the Atlantic Ocean near 36°50′N: petrology and geochemistry of basaltic rocks. Earth Planet. Sci. Lett. 24, 249–261.
Bougault, H. et al., 1984. Basalts From the Atlantic Crust West of the Barbados Ridge (Site-543, Leg-78a)—Geochemistry and Mineralogy. Initial Reports of the Deep Sea Drilling Project. 78(AUG), pp. 401–408.
Bryan, W.B., 1979. Regional variation and petrgenesis of basalt glasses from the FAMOUS area, Mid-Atlantic Ridge. J. Petrol. 20 (2), 293–325.
Bryan, W.B., Moore, J.G., 1977. Compositional variations of young basalts in mid-Atlantic Ridge rift valley near Lat 36°49′N. Geol. Soc. Am. Bull. 88 (4), 556–570.
Cannat, M., et al., 1999. Mid-Atlantic Ridge-Azores hotspot interactions: along-axis migration of a hotspt-derived event of enhanced magmatism 10 to 4 Ma ago. Earth Planet. Sci. Lett. 173, 257–269.
Chauvel, C., Blichert-Toft, J., 2001. A hafnium isotope and trace element perspective on melting of the depleted mantle. Earth Planet. Sci. Lett. 190 (3–4), 137–151.
Danyushevsky, L.V., Leslie, R.A.J., Crawford, A.J., Durance, P., 2004. Melt inclusions in primitive olivine phenocrysts: the role of localized reaction processes in the origin of anomalous compositions. J. Petrol. 45, 2531–2553.
Danyushevsky, L.V., Perfit, M.R., Eggins, S.M., Falloon, T.J., 2003. Crustal origin for coupled 'ultra-depleted' and 'plagioclase' signatures in MORB olivine-hosted melt inclusions: evidence from the Siqueiros Transform Fault, East Pacific Rise. Contrib. Mineral. Petrol. 144 (5), 619–637.
Detrick, R.S., Needham, H.D., Renard, V., 1995. Gravity-anomalies and crustal thickness variations along the Mid-Atlantic-Ridge between 33°N And 40°N. J. Geophys. Res. 100 (B3), 3767–3787.

Dosso, L., et al., 1999. The age and distribution of mantle heterogeneity along the Mid-Atlantic Ridge (31–41°N). Earth Planet. Sci. Lett. 170, 269–286.
Eason, D., Sinton, J., 2006. Origin of high-Al N-MORB by fractional crystallization in the upper mantle beneath the Galapagos Spreading Center. Earth Planet. Sci. Lett. 252, 423–436.
Escartin, J., Cannat, M., Pouliquen, G., Rabain, A., Lin, J., 2001. Crustal thickness of V-shaped ridges south of the Azores: interaction of the Mid-Atlantic Ridge (36°–39°N) and the Azores hot spot. J. Geophys. Res. 106 (B10), 21719–21735.
Frey, F.A., Walker, N., Stakes, D., Hart, S.R., Nielsen, R., 1993. Geochemical characteristics of basaltic glasses from the AMAR and FAMOUS axial valleys, Mid-Atlantic Ridge (36–37°N): petrogenetic implications. Earth Planet. Sci. Lett. 115, 117–136.
Gale, A., Escrig, S., Gier, E.J., Langmuir, C.H., Goldstein, S.L., 2011. Enriched basalts at segment centers: the Lucky Strike (37°17′N) and Menez Gwen (37°50′N) segments of the Mid-Atlantic Ridge. Geochem. Geophys. Geosyst. 12 (Q06016).
Gale, A., Dalton, C.A., Langmuir, C.H., Su, Y., Schilling, J-G., 2013, The mean composition of ocean ridge basalts, Geochem. Geophys. Geosyst., http://dx.doi.org/10.1002/ggge.20038.
Green, T.H., Blundy, J.D., Adam, J., Yaxley, G.M., 2000. SIMS determination of trace element partition coefficients between garnet, clinopyroxene and hydrous basaltic liquids at 2–7.5 GPa and 1080–1200 °C. Lithos 53 (3–4), 165–187.
Gurenko, A.A., Sobolev, A.V., 2006. Crust-primitive magma interaction beneath neovolcanic rift zone of Iceland recorded in gabbro xenoliths from Midfell, SW Iceland. Contrib. Mineral. Petrol. 151, 495–520.
Hebert, L.B., Montési, L.G.J., 2010. Generation of permeability barriers during melt extraction at mid-ocean ridges. Geochem. Geophys. Geosyst. 11, Q12008.
Hirth, G., Kohlstedt, D.L., 1996. Water in the oceanic upper mantle: implications for rheology, melt extraction and the evolution of the lithosphere. Earth Planet. Sci. Lett. 144 (1–2), 93–108.
Ingle, S., et al., 2010. Mechanisms of geochemical and geophysical variations along the western Galapagos Spreading Center. Geochem. Geophys. Geosyst. 11.
Ito, E., White, W.M., Gopel, C., 1987. The O, Sr, Nd and Pb isotope geochemistry of MORB. Chem. Geol. 62 (3–4), 157–176.
Ito, G., Mahoney, J.J., 2005a. Flow and melting of a heterogeneous mantle: 1. Method and importance to the geochemistry of ocean island and mid-ocean ridge basalts. Earth Planet. Sci. Lett. 230 (1–2), 29–46.
Ito, G., Mahoney, J.J., 2005b. Flow and melting of a heterogeneous mantle: 2. Implications for a chemically nonlayered mantle. Earth Planet. Sci. Lett. 230 (1–2), 47–63.
Jaques, A.L., Green, D.H., 1980. Anhydrous melting of periodotite at 0–15 Kb pressure and the genesis of tholeiitic basalts. Contrib. Mineral. Petrol. 73 (3), 287–310.
Kamenetsky, V., 1996. Methodology for the study of melt inclusions in Cr-spinel, and implications for parental melts of MORB from FAMOUS area. Earth Planet. Sci. Lett. 142, 479–486.
Kamenetsky, V., Crawford, A.J., 1998. Melt-peridotite reaction recorded in the chemistry of spinel and melt inclusions in basalt from 43°N, Mid-Atlantic Ridge. Earth Planet. Sci. Lett. 164, 345–352.
Katz, R.F., 2008. Magma dynamics with the enthalpy method: benchmark solutions and magmatic focusing at MORs. J. Petrol. 49 (12), 2099–2121.
Langmuir, C., et al., 1997. Hydrothermal vents near a mantle hot spot: the Lucky Strike vent field at 37°N on the Mid-Atlantic Ridge. Earth Planet. Sci. Lett. 148 (1–2), 69–91.
Langmuir, C.H., Bender, J.F., Bence, A.E., Hanson, G.N., Taylor, S.R., 1977. Petrogenesis of basalts from the FAMOUS area: Mid-Atlantic Ridge. Earth Planet. Sci. Lett. 36, 133–156.
Langmuir, C.H., Klein, E.M., Plank, T., 1992. Petrological systematics of mid-ocean ridge basalts: constraints on melt generation beneath ocean ridges. In: Phipps Morgan, J., Blackman, D.K., Sinton, J.M. (Eds.), Mantle Flow and Melt Generation at Mid-Ocean Ridges. Geophysical Monograph. American Geophysical Union, Washington, DC, pp. 183–280.
Laubier, M., Gale, A., Langmuir, C.H., 2012. Melting and crustal processes at the FAMOUS segment (mid-Atlantic Ridge): new insights from olivine-hosted melt inclusions from multiple samples. J. Petrol. 53 (4), 665–698.
Laubier, M., Schiano, P., Doucelance, R., Ottolini, L., Laporte, D., 2007. Olivine-hosted melt inclusions and melting processes beneath the FAMOUS zone (Mid-Atlantic Ridge). Chem. Geol. 240 (1–2), 129.
le Roex, A.P., Erlank, A.J., Needham, H.D., 1981. Geochemical and mineralogical evidence for the occurrence of at least three distinct magma types in the 'Famous' region. Contrib. Mineral. Petrol. 77, 24–37.
le Roex, A.P., Frey, F.A., Richardson, S.H., 1996. Petrogenesis of lavas from the AMAR Valley and Narrowgate region of the FAMOUS Valley, 36°–37°N on the Mid-Atlantic Ridge. Contrib. Mineral. Petrol. 124 (2), 167–184.
Longhi, J., 2002. Some phase equilibrium systematics of lherzolite melting: I. Geochem. Geophys. Geosyst. 3.
Melson, W.G., O'Hearn, T., Jarosewich, E., 2002. A data brief on the Smithsonian Abyssal Volcanic Glass Data File. Geochem. Geophys. Geosyst. 3 (4).
Michael, P.J., Chase, R.L., Allan, J.F., 1989. Petrologic and geologic variations along the Southern Explorer Ridge, Northeast Pacific Ocean. J. Geophys. Res. 94, 13895–13919.
Ondreas, H., Fouquet, Y., Voisset, M., RadfordKnoery, J., 1997. Detailed study of three contiguous segments of the Mid-Atlantic Ridge, South of the Azores (37°N to 38°30′ N), using acoustic imaging coupled with submersible observations. Mar. Geophys. Res. 19 (3), 231–255.
Ryan, W.B.F., et al., 2009. Global multi-resolution topography synthesis. Geochem. Geophys. Geosyst., 10.
Salters, V.J., Stracke, A., 2004. Composition of the depleted mantle. Geochem. Geophys. Geosyst. 5, Q05B07.
Schiffman, P., Zierenberg, R., Chadwick, W.W., Clague, D.A., Lowenstern, J., 2010. Contamination of basaltic lava by seawater: evidence found in a lava pillar from Axial Seamount, Juan de Fuca Ridge. Geochem. Geophys. Geosyst. 11.
Schilling, J.-G., 1975. Azores mantle blob: rare earth evidence. Earth Planet. Sci. Lett. 25, 103–115.
Schilling, J.G., et al., 1983. Petrologic and geochemical variations along the mid-Atlantic Ridge from 29°N to 73°N. Am. J. Sci. 283 (6), 510–586.
Shimizu, N., 1998. The geochemistry of olivine-hosted melt inclusions in a FAMOUS basalt ALV519-4-1. Phys. Earth Planet. Inter. 107, 183–201.
Sigurdsson, H., 1981. 1st-order major element variation in basalt glasses from the mid-Atlantic Ridge—29°N to 73°N. J. Geophys. Res. 86, 9483–9502.
Slater, L., McKenzie, D., Grönvold, K., Shimizu, N., 2001. Melt generation and movement beneath Theistareykir, NE Iceland. J. Petrol. 42, 321–354.
Sobolev, A.V., Hofmann, A.W., Nikogosian, I.K., 2000. Recycled oceanic crust observed in 'ghost plagioclase' within the source of Mauna Loa lavas. Nature 404, 986–989.
Sparks, D.W., Parmentier, E.M., 1991. Melt extraction from the mantle beneath spreading centers. Earth Planet. Sci. Lett. 105, 368–377.
Stakes, D.S., Shervais, J.W., Hopson, C.A., 1984. The volcanic–tectonic cycle of the Famous And Amar Valleys, Mid-Atlantic Ridge (36°47′N)—evidence from basalt glass and phenocryst compositional variations for a steady-state magma chamber beneath the valley Midsections, Amar-3. J. Geophys. Res. 89 (NB8), 6995–7028.
Sun, S.-s., McDonough, W.F., 1989. Chemical and isotopic systematics of oceanic basalts: implications for mantle composition and processes. In: Saunders, A.D., Norry, M.J. (Ed.), Magmatism in the Ocean Basins. Geological Society Special Publication, pp. 313–345.
White, W.M., Bryan, W.B., 1977. Sr-isotope, K, Rb, Cs, Sr, Ba, and rare-earth geochemistry of basalts from the FAMOUS area. Geol. Soc. Am. Bull. 88, 571–576.
White, W.M., Schilling, J.-G., 1978. The nature and origin geochemical variation in Mid-Atlantic Ridge basalts from the Central North Atlantic. Geochim. Cosmochim. Acta 42, 1501–1516.
Yang, T., Shen, Y., van der Lee, S., Solomon, S.C., Hung, S.H., 2006. Upper mantle structure beneath the Azores hotspot from finite-frequency seismic tomography. Earth Planet. Sci. Lett. 250 (1–2), 11–26.
Yu, D.M., Fontignie, D., Schilling, J.G., 1997. Mantle plume-ridge interactions in the Central North Atlantic: a Nd isotope study of Mid-Atlantic Ridge basalts from 30°N to 50°N. Earth Planet. Sci. Lett. 146 (1–2), 259–272.